Talanta 271 (2024) 125681

Contents lists available at ScienceDirect

Talanta

journal homepage: www.elsevier.com/locate/talanta

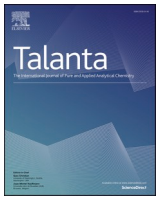

Intelligent monitoring of the available lead (Pb) and cadmium (Cd) in soil samples based on half adder and half subtractor molecular logic gates

Junhua Chen [a,b], Xu Wang [c], Yiwen Lv [b], Manjia Chen [b], Hui Tong [b], Chengshuai Liu [a,*]

[a] State Key Laboratory of Environmental Geochemistry, Institute of Geochemistry, Chinese Academy of Sciences, Guiyang, 550081, China
[b] National-Regional Joint Engineering Research Center for Soil Pollution Control and Remediation in South China, Guangdong Key Laboratory of Integrated Agro-Environmental Pollution Control and Management, Institute of Eco-Environmental and Soil Sciences, Guangdong Academy of Sciences, Guangzhou, 510650, China
[c] Institute of Quality Standard and Monitoring Technology for Agro-Products, Guangdong Academy of Agricultural Sciences, Guangzhou, 510640, China

ARTICLE INFO

Keywords:
Molecular logic gate
Intelligent sensing
DNA recognition
Heavy metal
Available Pb
Available Cd

ABSTRACT

The available heavy metals in soil samples can cause the direct toxicity on ecosystems, plants, and human health. Traditional chemical extraction and recombinant bacterial methods for the available heavy metals assay often suffer from inaccuracy and poor specificity. In this work, we construct half adder and half subtractor molecular logic gates with molecular-level biocomputation capabilities for the intelligent sensing of the available lead (Pb) and cadmium (Cd). The available Pb and Cd can cleave DNAzyme sequences to release the trigger DNA, which can activate the hairpin probe assembly in the logic system. This multifunctional logic system can not only achieve the intelligent recognition of the available Pb and Cd according to the truth tables, but also can realize the simultaneous quantification with high sensitivity, with the detection limits of 2.8 pM and 25.6 pM, respectively. The logic biosensor is robust and has been applied to determination of the available Pb and Cd in soil samples with good accuracy and reliability. The relative error (Re) between the logic biosensor and the DTPA + ICP-MS method was from −8.1 % to 7.9 %. With the advantages of programmability, scalability, and multicomputing capacity, the molecular logic system can provide a simple, rapid, and smart method for intelligent monitoring of the available Pb and Cd in environmental samples.

1. Introduction

Environmental contamination by heavy metals is a world-wide problem [1]. Lead (Pb) and cadmium (Cd) are the two highly toxic and widely distributed heavy metals in soil and sediment samples [2]. The heavy metal-induced toxicity on ecosystems, plants, and human health mainly depends on the available metal concentrations rather than the total amounts in the environment [3]. The available metals are usually defined as the soluble, ionic, and exchangeable forms that can interact with surrounding microorganisms and plant cells [4,5]. Due to many factors affecting the availability of heavy metals in soils [6], the development of innovative detection method for available heavy metal assay is challengeable and interesting.

Traditional techniques for the available Pb and Cd detection require sequential extraction procedures [4], such as DTPA method [7], BCR extraction [8], and Tessier protocol [9]. However, the strong acid extractant (HCl, HON_3, H_2SO_4 or $HClO_4$) used in the sequential extraction steps may alter the composition and nature of soil, making it greatly different from the soil required for plant growth [10–14]. Using strong acid chemicals for available heavy metal extraction was often confronted with the problems of excessive or insufficient extraction. Hence the amounts of heavy metals detected using those extraction techniques cannot truly reflect the portion of available heavy metals to the plants [15,16].

Another method for identifying available heavy metals is biological methods, such as recombinant bacterial biosensors [6]. The bacterial biosensors do not require extraction steps as the heavy metals are quantified relative to the concentrations experienced by the microorganisms, rather than relative to extraction techniques used for traditional chemical analysis [17,18]. However, the microbial whole-cell sensors often suffer from poor specificity. They may generate variable results depending on metal uptake and efflux activities which can substantially differ between each microorganism [4,19,20]. Another concern is that the assay time is relatively long as the microbial cultivation may take several days [21,22], which cannot meet the needs of rapid detection of available heavy metals. To address the limitations in

* Corresponding author.
E-mail address: liuchengshuai@vip.gyig.ac.cn (C. Liu).

https://doi.org/10.1016/j.talanta.2024.125681
Received 11 December 2023; Received in revised form 9 January 2024; Accepted 15 January 2024
Available online 17 January 2024

the chemical extraction techniques and bacterial biosensors, it is highly desirable to develop a rapid, convenient, selective, and reliable method for the detection of the available Pb and Cd in soil samples.

Deoxyribonucleic acid (DNA)-based biosensors have emerged as the promising tools in heavy metal detection [23]. The good stability, high specificity and scalability, and prominent biocompatibility make the DNA-based biosensors versatile in environmental monitoring [24]. For available heavy metal detection, DNA probes can be utilized as molecular recognition elements [25]. The available heavy metal-aptamer sequence interactions can change the DNA conformation to realize the signal conversion [26]. Another mechanism is that the available heavy metal-mediated cleavage of deoxyribozyme (DNAzyme) can release the trigger probe, which can be used to construct the sensing system [27,28]. Those reports focused on single heavy metal detection. Thus, it is interesting and challengeable to develop an intelligent sensing system of the simultaneous detection of available Pb and Cd in environmental samples.

Molecular logic gates, which can mimic computer microprocessors to execute binary Boolean operations and arithmetic processing, have attracted great attentions in recent years due to the multiple biocomputing capabilities [29]. The numbers 0 and 1 are used to encode the input and output signals according to the truth table [30,31]. The outputs of "true" (1, high vale) or "false" (0, low value) are depended on the input combinations [32]. Some interesting molecular logic gates with molecular-level biocomputation capabilities have been reported to fabricate smart sensing systems for intelligent diagnostics and molecular recognition, including AND, OR, XOR, INHIBIT, Half adder, Half subtractor, Keypad lock, and so on [33–40]. Most of these logic sensors utilized nucleic acids as inputs and focused on bioanalysis and clinic diagnosis [41–45]. There is little research on molecular logic gates used in environmental monitoring, especially using heavy metals as inputs. In this work, for the first time, we attempt to construct half adder and half subtractor logic gates using the available Pb and Cd as inputs. Pb DNAzyme and Cd DNAzyme were used to recognize the available Pb and Cd, respectively. The logic gate biosensor also can realize the simultaneous quantification with high sensitivity. This logic system can provide an intelligent sensing strategy for the available Pb and Cd monitoring in soil samples.

2. Experimental section

2.1. Chemicals and materials

DNA probes were ordered from Shanghai Sangon Biotechnology Co., Ltd. (Shanghai, China) and the sequences were listed in Tables S1–S6 (Supporting Information). Streptavidin (SA)-coated magnetic beads (MB, 1 μM in diameter) were purchased from Shanghai Aladdin Biochemical Technology Co., Ltd (Shanghai, China). Other chemicals were purchased from Sigma-Aldrich (Merck KGaA, Darmstadt, Germany). Milli-Q water (18.2 MΩ/cm) was used in the experiments.

2.2. Procedures for logic gate operation

All DNA probes were separately heated at 95 °C for 10 min and then gradually cooled to room temperature at a constant rate of 1 °C/min 100 nM biotinylated S1 and S2 were separately added to the SA-coated MB solution (200 μL, 1.2 mg/mL) and incubated at room temperature for 30 min with gentle shaking. After magnetic separation and washing three times with the washing buffer (20 mM PBS, 0.01 % Tween-20, pH 7.4), the resulting MB-S1 and MB-S2 conjugates were redispersed in the working buffer (20 mM Tris-Ac, 150 mM NaAC, pH 6.8). 120 nM D1 and 120 nM D2 were added to MB-S1 and MB-S2, respectively. After incubation at room temperature for 30 min, the mixture was separated by magnet and the obtained MB-S1-D1 and MB-S2-D2 conjugates were dispersed in the working buffer. 10 nM Pb and 10 nM Cd were used as the two inputs in the logic experiments. After the addition of heavy metals to MB-S1-D1 and MB-S2-D2 conjugates and incubated at room temperature for 40 min, the supernatant was transferred to 150 nM H0, H1, H2, H3 or H4 solution and further incubated for 60 min at room temperature. The fluorescence spectra of the solution were recorded by the SpectraMax i3x (Molecular Devices, San Jose, USA).

2.3. Soil sample analysis

The soil samples were collected from an agricultural field near South China Botanical Garden (Guangzhou, China). After air-drying, the soil was sieved to pass through 0.15 mm mesh and homogenized thoroughly. We used two methods to detect the available Pb and Cd in soil samples: DTPA method and logic sensor. For the DTPA method, the DTPA extracting solution was prepared to contain 10 mM $CaCl_2$, 100 mM triethanolamine, and 5 mM DTPA in deionized water matrix. The pH of the extracting solution was adjusted to 7.3 by addition of HCl. 10 g soil and 20 mL DTPA extracting solution were mixed and shaken on a horizontal shaker at 160 cycles/min for 2h. After centrifugation at 5000 rpm for 10 min, the supernatant was filtered through Whatman No. 42 filter paper. The filtrates were used to analyze the available Pb and Cd using inductively coupled plasma mass spectrometer (ICP-MS). For the logic sensor, the homogenized soil samples were added to the working buffer containing MB-S1-D1 or MB-S2-D2 conjugates and incubated at room temperature for 40 min. After magnetic separation, the supernatant was transferred to the working buffer containing H0, H1, H2, H3, and H4. Other procedures were the same as described in the section of "Procedures for logic gate operation".

2.4. Native polyacrylamide gel electrophoresis (PAGE)

12 % hydrogel was used to carry out the native PAGE experiments and the details of the PAGE procedures were listed in the Supporting Information.

3. Results and discussion

3.1. DNAzyme recognition of available heavy metals

The Pb DNAzyme (S1-D1) and Cd DNAzyme (S2-D2) were used to recognize the available Pb and Cd, respectively. We used the fluorescence spectra to verify the DNAzyme responses to the available Pb and Cd. As show in Fig. 1A, the probe S1 was modified with BHQ and the probe D1 was modified with FAM. In the absence of Pb, the Pb DNAzyme (S1-D1) displayed a weak fluorescence signal due to the fluorescence quenching between BHQ and FAM (black curve). The results indicated that the Pb DNAzyme was stable in the solution without the target Pb. In the presence of Pb, D1 will be cleaved into two parts to generate a high fluorescence signal (green curve), indicating that the strand (5–6*) was released. This phenomenon proved that the available Pb can indeed cleave the Pb DNAzyeme at the rA position. We also verified the feasibility of cleavage reaction of the available Cd to the Cd DNAzyme. As show in Fig. 1B, in the absence of Cd, the Cd DNAzyme (S2-D2) displayed a weak fluorescence signal due to the fluorescence quenching between S2 and D2. In the presence of Cd, D2 will be cleaved into two parts to generate a high fluorescence signal, indicating that the strand (6-5) was released. The above results successfully verified that the available Pb and Cd can cleave the DNAzyme probes, thereby releasing the trigger DNA for subsequent assembly reactions.

3.2. Construction of half adder logic gate

This logic system contains Pb DNAzyme (S1-D1), Cd DNAzyme (S2-D2), H0, H1 (modified with FAM and BHQ), H2, H3 (modified with Cy5 and BHQ), and H4. For the input definition, the presence and absence of Pb and Cd were set as 1 and 0, respectively. For the output definition, the high and low fluorescence signals were set as 1 and 0, respectively. Fig. 2

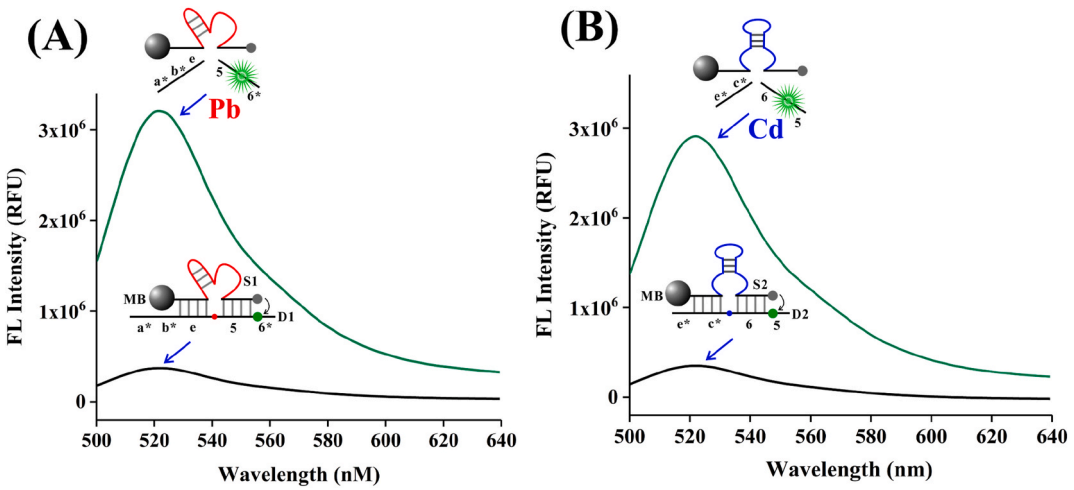

Fig. 1. (A) Fluorescence responses of the Pb DNAzyme in the presence (green curve) and absence (black curve) of Pb. S1 was modified with BHQ. D1 was modified with FAM. (B) Fluorescence responses of the Cd DNAzyme in the presence (green curve) and absence (black curve) of Cd. S2 was modified with BHQ. D2 was modified with FAM.

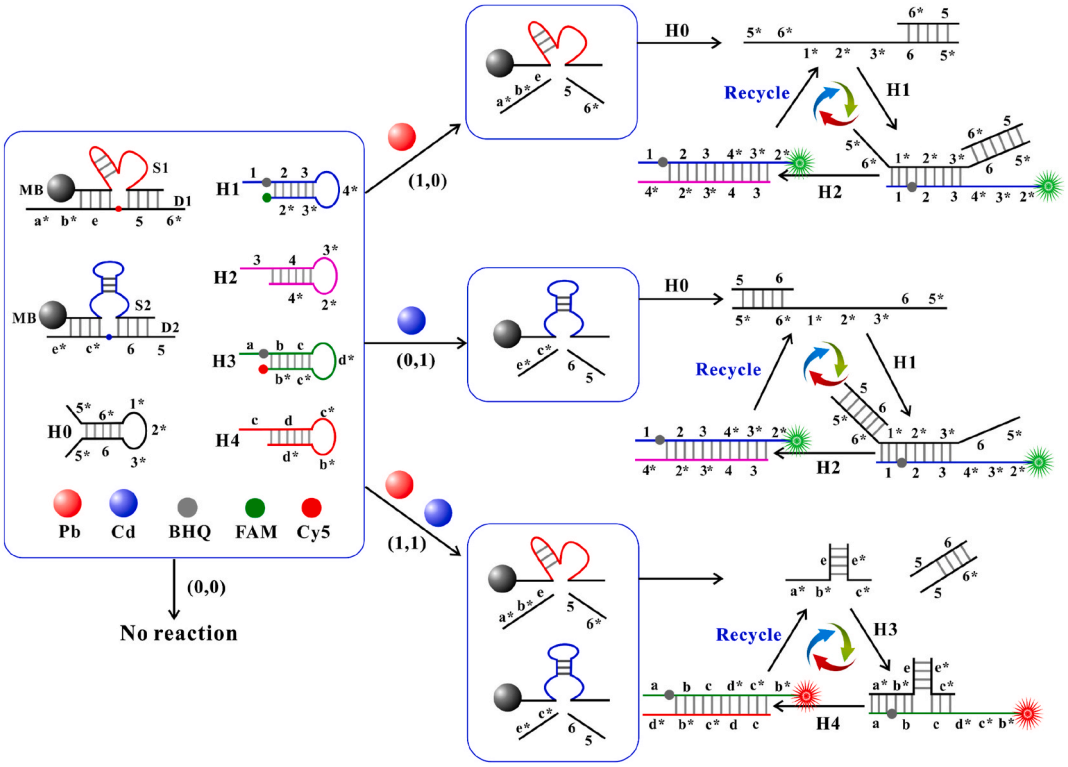

Fig. 2. Schematic illustration of half adder logic gate operation. Pb and Cd are used as the two inputs. Pb DNAzyme (S1-D1), Cd DNAzyme (S2-D2), H0, H1 (modified with FAM and BHQ), H2, H3 (modified with Cy5 and BHQ), and H4 are employed as the sensing elements. MB, magnetic bead modified with SA.

shows the construction of the half adder logic gate, which can be implemented by integration of an XOR logic gate and an AND logic gate in parallel. The fabrication of XOR logic gate was show in Figs. S1 and S2 (Supporting Information). The fabrication of AND logic gate was show in Figs. S3 and S4 (Supporting Information).

In the absence of any input (0,0), the substrate chains (D1 and D2) were blocked by the enzyme strands (S1 and S2). All the hairpin probes kept the closed states and only weak fluorescence signals can be observed due to the close proximity between FAM/Cy5 and BHQ.

In the presence of either Pb or Cd (1,0 or 0,1), the heavy metal-DNAzyme interactions will cleave the enzyme strands (S1 or S2) at the rA position. After magnetic separation, the released 5–6* fragment or 5–6 fragment can open H0 through toehold-mediated strand displacement reaction (5–6* hybridizes with 5*-6 of H0 or 5–6 fragment hybridizes with 5*-6* of H0). The opened H0 contains the free 1*-2*-3* fragment, which can be used as the trigger strand to activate the assembly process between H1 and H2. Using the domain 1* as the binding toehold, the trigger strand (1*-2*-3*) can open H1 and the domain 3* in H1 thus will be exposed. Then, H2 will hybridize with H1 through toehold-mediated strand reaction to form the H1–H2 product. At the same time, the trigger strand will be released and recycled to trigger the new assembly reaction between H1 and H2. Through continuous signal amplification, the separation of FAM and BHQ will generate a high FAM fluorescence signal, which encodes an XOR logic gate.

In the presence of both Pb and Cd (1,1), the released 5–6* and 5–6 fragments will hybridize with each other to generate a favored duplex DNA, which prohibits the opening of H0. Thus, the interactions between H1 and H2 cannot happen and only weak FAM fluorescence signals can be observed. At the same time, the released a*-b*-e fragment hybridizes with the c*-e* fragment to form the a*-b*-e-e*-c* complex, in which the a*-b* domain and the c* domain get close enough to form the free a*-b*-c* trigger strand, which can then activate the assembly reaction between H3 and H4. The formed H3–H4 products produce a high Cy5 fluorescence signal to indicate an AND gate operation.

Fig. 3A shows the FAM fluorescence spectra of the half adder logic operation. Fig. 3B shows the Cy5 fluorescence spectra of the half adder logic operation. The corresponding fluorescence intensities of FAM and Cy5 are recorded at 525 nm and 670 nm, respectively (Fig. 3C). The truth table of the half adder logic gate is given in Fig. 3D. The logic circuitry is given in Fig. 3E. Triggered by the same inputs (Pb and Cd), FAM-related XOR gate and Cy5-related AND gate were produced in parallel, coding for a SUM (S) digit and a CARRY (C) digit, respectively.

3.3. Construction of half subtractor logic gate

The operation principle of the half subtractor is illustrated in Fig. 4. A half subtractor is composed of parallel XOR and INHIBIT logic gates to generate a DIFFERENCE (D) output and a BORROW (B) output, respectively. The fabrication of XOR logic gate was show in Figs. S1 and S2 (Supporting Information). The fabrication of INHIBIT logic gate was show in Figs. S5 and S6 (Supporting Information). The fabrication of OR logic gate was show in Figs. S7 and S8 (Supporting Information).

In the absence of any input (0,0), no cleavage reaction was happened and the hairpin probes H1 (modified with FAM and BHQ) and H3 (modified with Cy5 and BHQ) remain closed. The low FAM and Cy5 fluorescence signals give an output of 0.

In the presence of either Pb or Cd (1,0 or 0,1), D1 and D2 will be cleaved and the released 5–6* or 5–6 fragments can open H0 to free 1*-2*-3* domain, which can activate the assembly reaction between H1 and H2. The high FAM fluorescence signals coding the XOR logic gate give an output of 1. At the same time, the (0,1) state will produce a free a*-b*-c* fragment, which can trigger the H3–H4 binding and produce a high Cy5 fluorescence signal. The Cy5 signal was used to indicate the INHIBIT logic gate.

In the presence of both Pb and Cd (1,1), two kinds of duplex (5–6/5-6* and a-b-c/a*-b-*c*) will be formed. H1 and H3 kept the closed states and only low FAM and Cy5 signals can be generated.

Fig. 5A shows the FAM fluorescence spectra of the half subtractor logic operation. Fig. 5B shows the Cy5 fluorescence spectra of the half subtractor logic operation. The corresponding fluorescence intensities of FAM and Cy5 are recorded at 525 nm and 670 nm, respectively (Fig. 5C). The truth table of the half subtractor logic gate is given in Fig. 5D. The logic circuitry is given in Fig. 5E. Triggered by the same inputs (Pb and Cd), FAM-related XOR gate and Cy5-related INHIBIT gate were produced in parallel, coding for a DIFFERENCE (D) digit and a BORROW (B) digit, respectively.

3.4. Fluorescence and electrophoresis characterization of the logic gate

The fluorescence responses and native PAGE experiments were used to verify the feasibility of the logic system. We first verified the hairpin assembly between H1 and H2 using the strand (1*-2*-3*) as a trigger DNA. As shown in Fig. 6A, H1 and H2 displayed a weak fluorescence signal. When incubation of 1*-2*-3* strand (T) and H1, the fluorescence

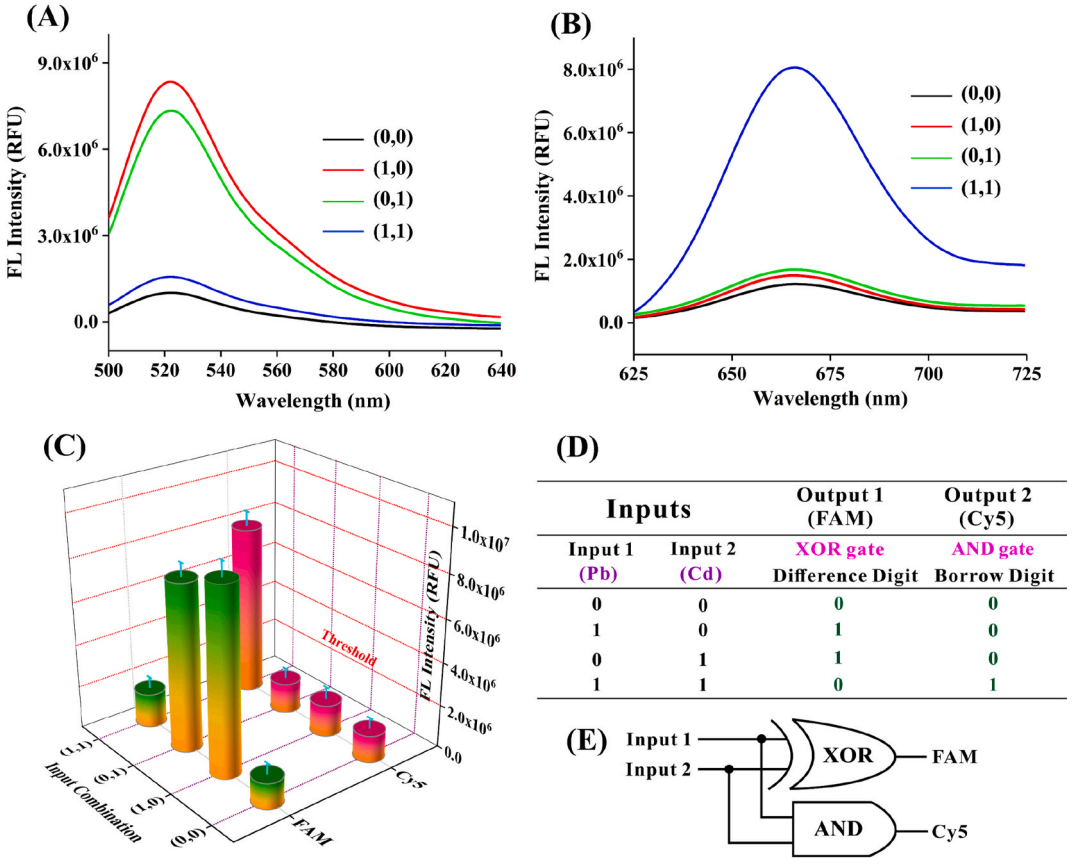

Inputs		Output 1 (FAM)	Output 2 (Cy5)
Input 1 (Pb)	Input 2 (Cd)	XOR gate Difference Digit	AND gate Borrow Digit
0	0	0	0
1	0	1	0
0	1	1	0
1	1	0	1

Fig. 3. (A) Fluorescence spectra (FAM) of half adder logic gate toward different input combinations. (B) Fluorescence spectra (Cy5) of half adder logic gate toward different input combinations. (C) Histogram of the corresponding fluorescence intensities at 525 nm and 670 nm. The threshold fluorescence intensity is set at 2×10^6. (D) Truth table of half adder logic gate (E) Diagram of electronic half adder logic circuit.

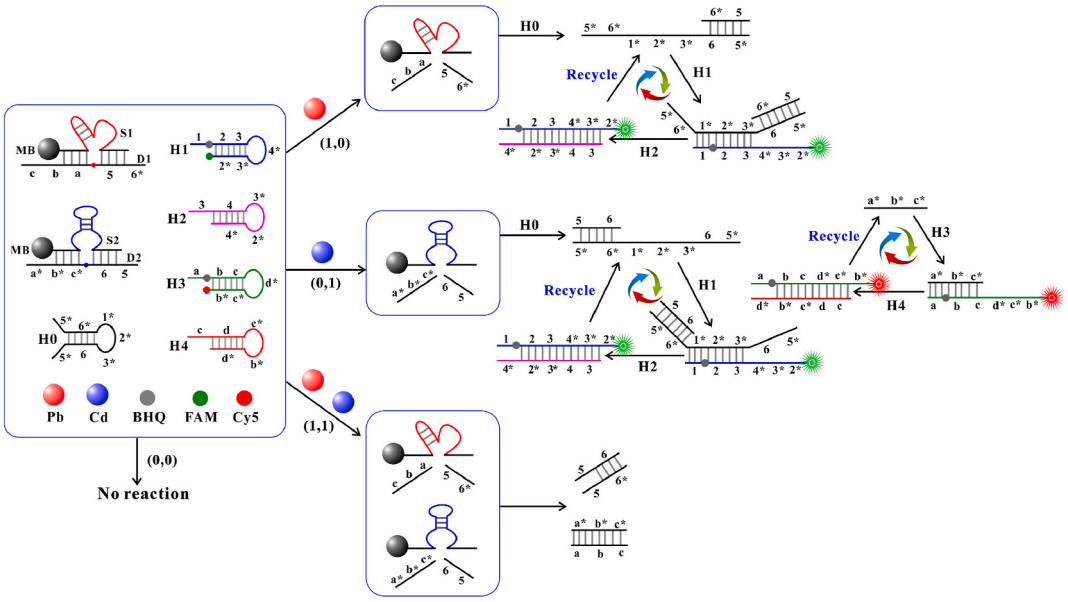

Fig. 4. Schematic illustration of half subtractor logic gate operation. Pb and Cd are used as the two inputs. Pb DNAzyme (S1-D1), Cd DNAzyme (S2-D2), H0, H1 (modified with FAM and BHQ), H2, H3 (modified with Cy5 and BHQ), and H4 are employed as the sensing elements. MB, magnetic bead modified with SA.

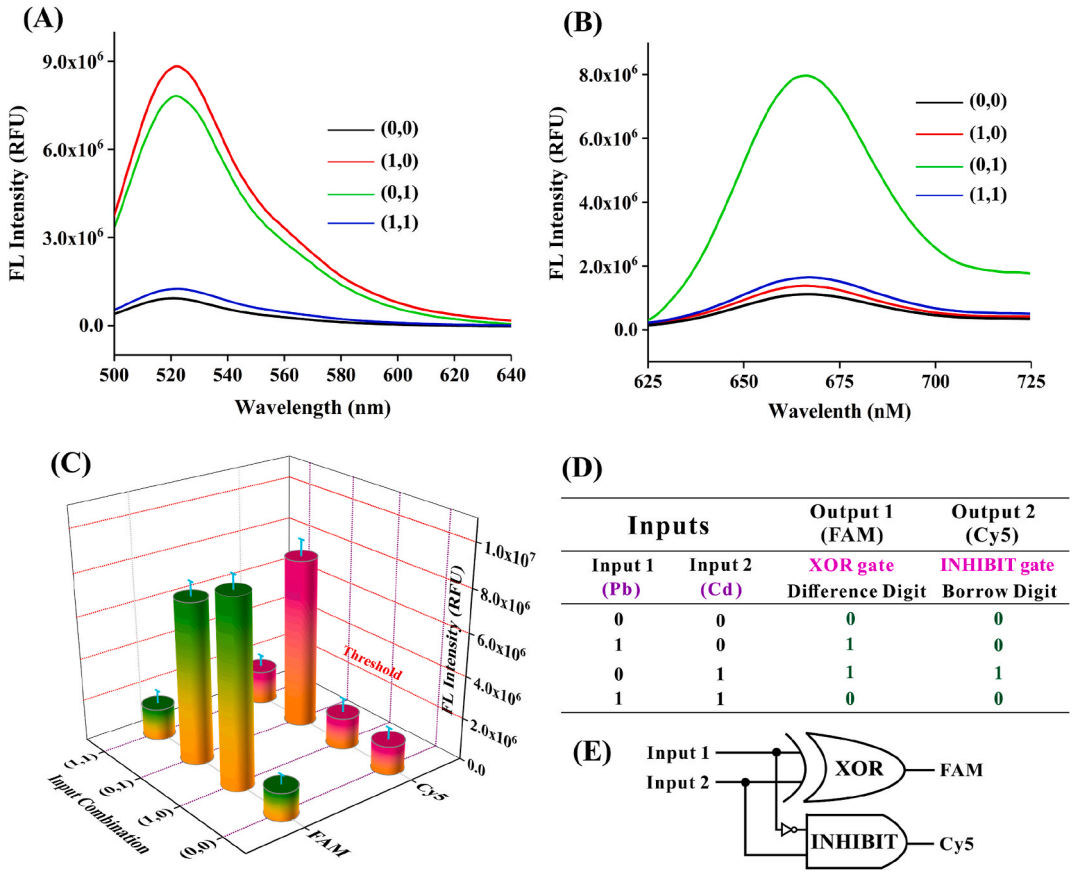

Inputs		Output 1 (FAM)	Output 2 (Cy5)
Input 1 (Pb)	Input 2 (Cd)	XOR gate Difference Digit	INHIBIT gate Borrow Digit
0	0	0	0
1	0	1	0
0	1	1	1
1	1	0	0

Fig. 5. (A) Fluorescence spectra (FAM) of half subtractor logic gate toward different input combinations. (B) Fluorescence spectra (Cy5) of half adder logic gate toward different input combinations. (C) Histogram of the corresponding fluorescence intensities at 525 nm and 670 nm. The threshold fluorescence intensity is set at 2×10^6. (D) Truth table of half subtractor logic gate (E) Diagram of electronic half subtractor logic circuit.

signal was recovered due to the formation of the T-H1 complex. In the presence of T, H1, and H2, a high fluorescence signal can be observed, indicating that the cyclic assembly between H1 and H2 was indeed happened and the product of H1–H2 was formed. The hairpin assembly between H3 and H4 was also confirmed in Fig. 6B. The trigger DNA (a*-b*-c*) can open H3 to give a fluorescence signal and the formed H3–H4 product yield a high fluorescence response.

The PAGE experiments were also carried out to verify the assembly

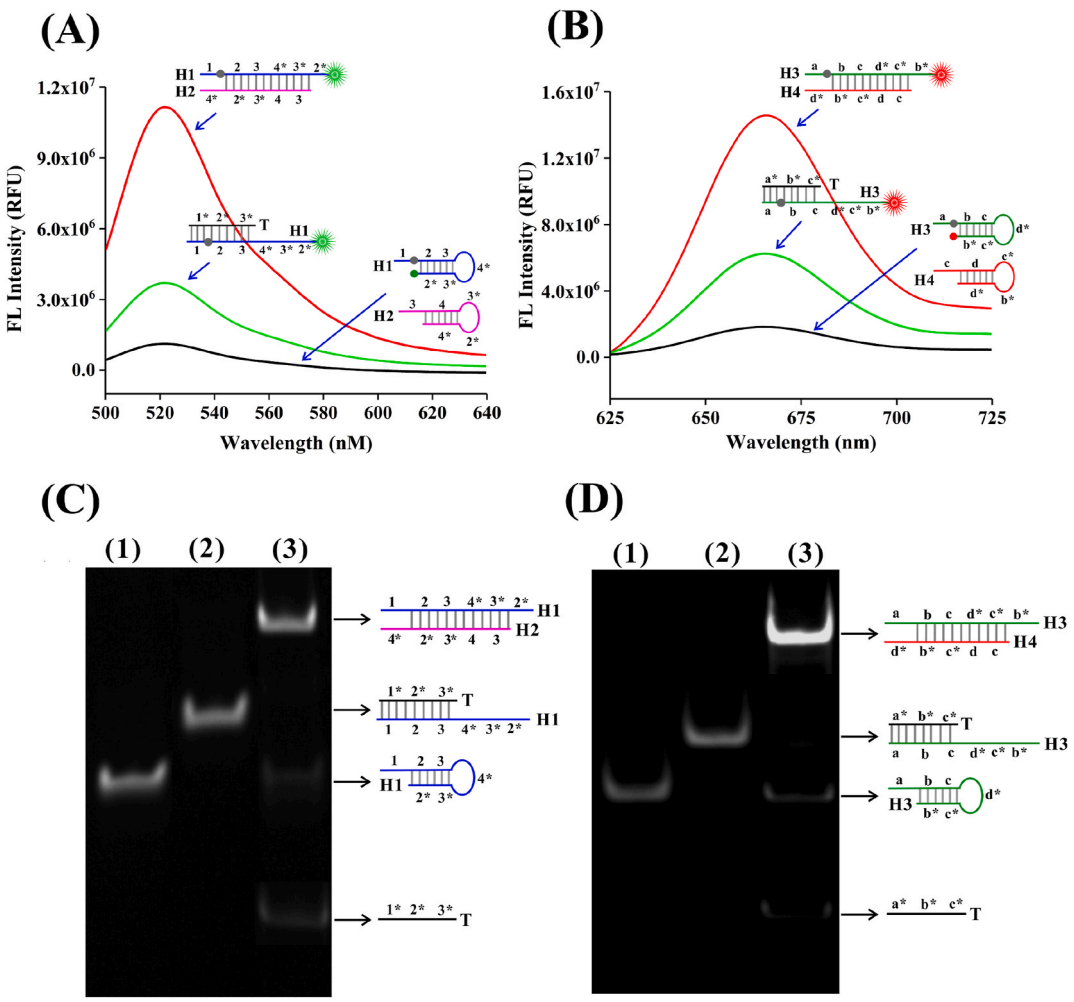

Fig. 6. (A) Fluorescence responses of the hairpin assembly between H1 and H2. Black curve: Hairpin probes H1 and H2. Green curve: Hairpin probe H1 + the trigger strand (1*-2*-3*). Red curve: Hairpin probes H1 and H2 + the trigger strand (1*-2*-3*). (B) Fluorescence responses of the hairpin assembly between H3 and H4. Black curve: Hairpin probes H3 and H4. Green curve: Hairpin probe H3 + the trigger strand (a*-b*-c*). Red curve: Hairpin probes H1 and H2 + the trigger strand (a*-b*-c*). (C) PAGE verification of the hairpin assembly between H1 and H2. Lane 1: H1. Lane 2: T (1*-2*-3*) + H1. Lane 3: T (1*-2*-3*) + H1 + H2. (D) PAGE verification of the hairpin assembly between H3 and H4. Lane 1: H1. Lane 2: T (a*-b*-c*) + H1. Lane 3: T (a*-b*-c*) + H1 + H2.

between H1 and H2 and the results were shown in Fig. 6C. The lane 1 corresponded to H1. The band in lane 2 represented the T-H1 complex. After mixing T, H1, and H2 together, a band with reduced mobility could be observed in lane 3, indicating that the H1–H2 product was formed. Similar situation can also be observed in the assembly between H3 and H4 (Fig. 6D).

3.5. Quantitative analysis of Pb and Cd

We used the half subtractor logic gate as an example to test the analytical performance of the logic system for Pb and Cd detection. In the presence of Pb, D1 probe will be cleaved into two parts, which can be used to trigger the assembly between H1 and H2. The generated FAM fluorescence signals can be used to quantitate the Pb concentration. As show in Fig. 7A and B, with the increase of Pb concentration from 0 to 10 μM, the FAM fluorescence signals increased accordingly. The fluorescence intensity at 525 nm is proportional to the logarithm of Pb concentration in the range from 10 pM to 1 μM. The detection limit (LOD) was calculated to be 2.8 pM based on 3S/N. In the presence of Cd, D2 probe will be cleaved into two parts and the released a*-b*-c* can activate the H3–H4 assembly to yield Cy5 signals, which can be used to quantitate the Cd concentration. As show in Fig. 7C and D, with the increase of Cd concentration from 0 to 100 μM, the Cy5 fluorescence signals increased accordingly. The fluorescence intensity at 670 nm is proportional to the logarithm of Cd concentration in the range from 100 pM to 10 μM. The detection limit (LOD) was calculated to be 25.6 pM based on 3S/N. Thus, our constructed logic sensing system can be used to quantitate the Pb and Cd concentrations with high sensitivity. Compared with some previously reported Pb and Cd sensors (Table S7, Supporting Information), our constructed logic gate biosensor displayed a superior detection sensitivity. Such high sensitivity can be attributed to the excellent sensing performance of the logic biocomputation capability.

3.6. Selectivity test and real sample analysis

The selectivity of the logic system is based on the specific cleavage reaction between heavy metal and DNAzyme. The Pb DNAzyme exhibits excellent specificity for Pb (Fig. S9, Supporting Information) and the control heavy metals (Zn, Ni, Co, Hg, Cu, Cr, Fe, Mn, Sn, Al, and Ag) did not affect the logic sensor for Pb assay. The specificity of the Cd DNAzyme for Cd is also excellent (Fig. S10, Supporting Information) and the control heavy metals (Zn, Ni, Co, Hg, Cu, Cr, Fe, Mn, Sn, Al, and Ag) did not interfere with Cd detection.

The practicability of the logic system was validated by measuring the available Pb and Cd in soil samples. The soil samples were first extracted

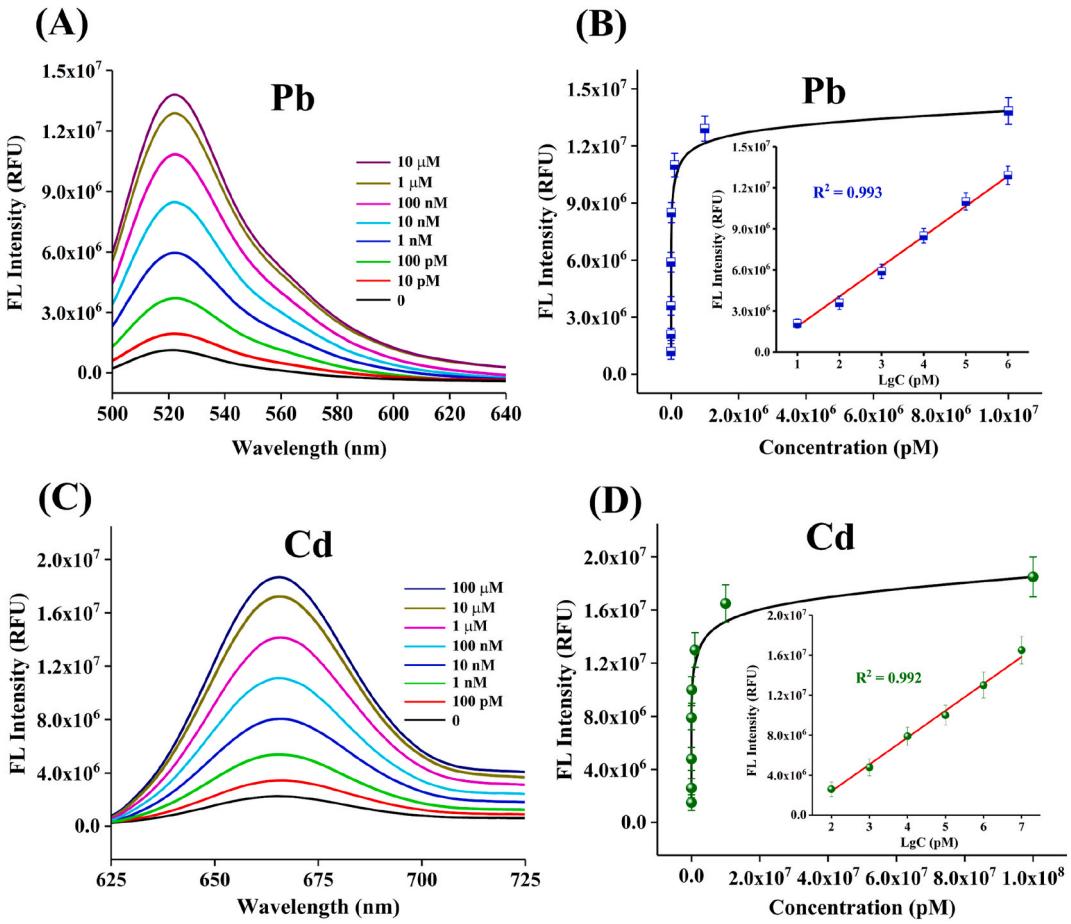

Fig. 7. (A) Fluorescence spectra of the half subtractor logic gate upon the addition of different concentrations of Pb. (B) Plots of the fluorescence intensity at 525 nm as a function of the Pb concentration. Inset: Linear relationship between the fluorescence intensity and the logarithm of Pb concentration in the range from 10 pM to 1 μM. (C) Fluorescence spectra of the half subtractor logic gate upon the addition of different concentrations of Cd. (D) Plots of the fluorescence intensity at 670 nm as a function of the Cd concentration. Inset: Linear relationship between the fluorescence intensity and the logarithm of Cd concentration in the range from 100 pM to 10 μM.

by the conventional DTPA method and then quantified by the ICP-MS method. At the same time, the logic sensor was also used to detect the available Pb and Cd in soil samples. As shown in Table 1, the relative standard deviation (RSD) of the logic sensor detection was below 6 %. The relative error (Re) between the logic sensor and the DTPA + ICP-MS method was from −8.1 % to 6.1 % for the available Pb and from −3.8 % to 7.9 % for the available Cd. These results indicated that our proposed logic system is robust and can be used to detect the available Pb and Cd in soil samples with good accuracy and reliability.

Table 1
Detection of the available Pb and Cd in soil samples using the logic sensor and the conventional DTPA + ICP-MS method.

	Samples	ICP-MS[a]	Logic sensor[b]	RSD[c] (%)	Re[d] (%)
Soil 1#	Pb	12.67 nM	11.64 nM	4.1	−8.1
	Cd	8.62 nM	8.98 nM	3.6	4.2
Soil 2#	Pb	29.45 nM	31.26 nM	4.5	6.1
	Cd	42.86 nM	44.75 nM	4.2	4.4
Soil 3#	Pb	84.55 nM	81.32 nM	5.3	−3.8
	Cd	28.03 nM	30.27 nM	5.6	7.9
Soil 4#	Pb	187.61 nM	190. 56 nM	4.8	1.6
	Cd	183. 89 nM	178. 63 nM	5.4	−2.9
Soil 5#	Pb	286.56 nM	298. 58 nM	4.6	4.2
	Cd	159.24 nM	169. 27 nM	5.2	6.3

[a] The available Pb and Cd was extracted by DTPA method and detected by inductively coupled plasma mass spectrometer (ICP-MS).
[b] Logic sensor method (n = 3).
[c] Relative standard deviation (n = 3).
[d] Relative error: Proposed logic sensor *vs.* ICP-MS.

To further verify the logic operations of the logic gates in real sample, we used the half adder gate as an example to examine the logic signals in soil samples. The ICP-MS confirmed Pb (22.8 nM) and Cd (54.6 nM) samples were used to perform the half adder gate. As shown in Fig. S11 (Supporting Information), in the (0,0) state, only weak FAM and Cy5 signals can be observed. The SUM and CARRY outputs read 0. In the (1,0) and (0,1) states, a high FAM and a low Cy5 signals can be observed. The SUM outputs read 1 and the CARRY outputs read 0. In the (1,1) state, a low FAM and a high Cy5 signals can be observed. The SUM output reads 0 and the CARRY output reads 1. These results indicated that the half adder gate can work even in complex samples with satisfactory logic functions. At the same time, we also tested the AND logic gate operations in real soil samples. Fig. S12A (Supporting Information) shows the fluorescence spectra of the AND logic operation in real soil samples. Fig. S12B shows the corresponding fluorescence intensity at 525 nm. The truth table of the AND logic gate in given in Fig. S12C. The logic circuitry is given in Fig. S12D. In AND logic gate, the output is 1 only if both inputs are 1. These results indicated that the AND logic gate can also work in complex samples with satisfactory logic functions.

4. Conclusions

In conclusion, we have successfully constructed half adder and half subtractor logic gates using the available Pb and Cd as inputs based on

DNAzyme recognition and hairpin probes assembly. The half adder logic gate can be implemented by integration of an XOR logic gate and an AND logic gate in parallel. The half subtractor logic gate is composed of parallel XOR and INHIBIT logic gates. Through the rational design of the probe hybridization reactions, multiple logic functions can be realized according to the truth tables. The logic system can also realize the quantitative detection of the available Pb and Cd with high sensitivity, with the LOD of 2.8 pM and 25.6 pM, respectively. The logic system is robust and has been applied to the sensing of the available Pb and Cd in soil samples. The relative error (Re) between the logic biosensor and the DTPA + ICP-MS method was from −8.1 % to 7.9 %. In the logic biosensor, using DNA probes as molecular recognition elements can more accurately reflect the real concentrations of the available heavy metals in the detection system. Our developed logic biocomputing system can provide a reliable, simple, rapid, and smart method for intelligent monitoring of the available Pb and Cd in soil samples. Compared with traditional chemical extraction methods, the special advantage is that the logic operation is simple and the detection can be finished by mixing the DNA probes without complex extraction steps. This study not only expands the applications of logic gates in environmental monitoring using the available heavy metals as inputs, but also will inspire researchers to create more intricate and intelligent biocomputing devices.

CRediT authorship contribution statement

Junhua Chen: Writing – original draft, Methodology, Investigation, Conceptualization, Writing – review & editing. **Xu Wang:** Methodology, Investigation, Formal analysis. **Yiwen Lv:** Methodology, Data curation. **Manjia Chen:** Validation, Resources, Methodology. **Hui Tong:** Validation, Methodology, Data curation. **Chengshuai Liu:** Writing – review & editing, Project administration, Funding acquisition.

Declaration of competing interest

The authors declare that they have no known competing financial interests or personal relationships that could have appeared to influence the work reported in this paper.

Data availability

Data will be made available on request.

Acknowledgements

This work was supported by the National Natural Science Foundations of China (42330712, 42377454, and 42025705), Guizhou Province High-level Talent Project (GCC[2022]002-1), GDAS'Project of Science and Technology Development, China (2019GDASYL-0103048), and the National Key Research and Development Program of China (2020YFC1808500).

Appendix A. Supplementary data

Supplementary data to this article can be found online at https://doi.org/10.1016/j.talanta.2024.125681.

References

[1] E. Malematja, T.G. Manyelo, N.A. Sebola, S.D. Kolobe, M. Mabelebele, The accumulation of heavy metals in feeder insects and their impact on animal production, Sci. Total Environ. 885 (2023) 163716.
[2] J. Dong, L. Wen, D. Zhao, H. Yang, J. Zhao, Z. Hu, Y. Ma, C. Hou, D. Hou, Flexible carbon fiber cloth supports decorated with cerium metal-organic frameworks and multi-walled carbon nanotubes for simultaneous on-site detection of Cd^{2+} and Pb^{2+} in food and water samples, Food Chem. 419 (2023) 135869.
[3] E.A. Ibrahim, M.A.A. El-Sherbini, E.M. Selim, Effects of biochar on soil properties, heavy metal availability and uptake, and growth of summer squash grown in metal-contaminated soil, Sci. Hortic. 301 (2022) 111097.
[4] C. Rensing, R.M. Maier, Issues underlying use of biosensors to measure metal bioavailability, Ecotoxicol. Environ. Saf. 56 (2003) 140–147.
[5] H. Gao, G.F. Koopmans, J. Song, J.E. Groenenberg, X. Liu, R.N.J. Comans, L. Weng, Evaluation of heavy metal availability in soils near former zinc smelters by chemical extractions and geochemical modelling, Geoderma 423 (2022) 115970.
[6] O. Bondarenko, T. Rolova, A. Kahru, A. Ivask, Bioavailability of Cd, Zn and Hg in soil to nine recombinant luminescent metal sensor bacteria, Sensors 8 (2008) 6899–6923.
[7] W.L. Lindsay, W.A. Norvell, Development of a DTPA soil test for zinc, iron, manganese, and copper, Soil Sci. Soc. Am. J. 42 (1978) 421–428.
[8] A.M. Ure, P. Quevauviller, H. Muntau, B. Griepink, Speciation of heavy metals in soils and sediments. An account of the improvement and harmonization of extraction techniques undertaken under the auspices of the BCR of the Commission of the European Communities, Int. J. Environ. Anal. Chem. 51 (1993) 135–151.
[9] A. Tessier, P.G.C. Campbell, M. Bisson, Sequential extraction procedure for the speciation of particulate trace metals, Anal. Chem. 51 (1979) 844–851.
[10] F. Mehrabi, M. Ghaedi, E.A. Dil, Magnetic nanofluid based on hydrophobic deep eutectic solvent for efficient and rapid enrichment and subsequent determination of cinnamic acid in juice samples: vortex-assisted liquid-phase microextraction, Talanta 260 (2023) 124581.
[11] E.A. Dil, M. Ghaedi, F. Mehrabi, L. Tayebi, Highly selective magnetic dual template molecularly imprinted polymer for simultaneous enrichment of sulfadiazine and sulfathiazole from milk samples based on syringe-to-syringe magnetic solid-phase microextraction, Talanta 232 (2021) 122449.
[12] E.A. Dil, M. Ghaedi, A. Asfaram, L. Tayebi, Simultaneous selective enrichment of methylparaben, propylparaben, and butylparaben from cosmetics samples based on syringe-to-syringe magnetic fluid phase microextraction, Talanta 221 (2021) 121547.
[13] F. Mehrabi, M. Ghaedi, Magnetic nanofluid based on green deep eutectic solvent for enrichment and determination of chloramphenicol in milk and chicken samples by high-performance liquid chromatography-ultraviolet: optimization of microextraction, J. Chromatogr. A 1689 (2023) 463705.
[14] E.A. Dil, M. Ghaedi, A. Asfaram, F. Mehrabi, A. Shokrollahi, A.A. Matin, L. Tayebi, Magnetic dual-template molecularly imprinted polymer based on syringe-to-syringe magnetic solid-phase microextraction for selective enrichment of p-coumaric acid and ferulic acid from pomegranate, grape, and orange samples, Food Chem. 325 (2020) 126902.
[15] S.H. Lin, S.L. Lai, H.G. Leu, An improved method for determination of heavy metal bioavailability in contaminated soil, Environ. Technol. 22 (2001) 731–739.
[16] W. Zhou, J. Zhang, M. Zou, X. Du, Y. Zhang, Y. Yang, J. Li, The detection and monitoring of available heavy metal content in soil: a review, Chin. J. Eco-Agric. 25 (2017) 605–615.
[17] C. Liu, H. Yu, B. Zhang, S. Liu, C. Liu, F. Li, H. Song, Engineering whole-cell microbial biosensors: design principles and applications in monitoring and treatment of heavy metals and organic pollutants, Biotechnol. Adv. 60 (2022) 108019.
[18] T. Teng, W.E. Huang, G. Li, X. Wang, Y. Song, X. Tang, D. Dawa, B. Jiang, D. Zhang, Application of magnetic-nanoparticle functionalized whole-cell biosensor array for bioavailability and ecotoxicity estimation at urban contaminated sites, Sci. Total Environ. 896 (2023) 165292.
[19] M. Almendras, M. Carballa, L. Diels, K. Vanbroekhoven, R. Chamy, Prediction of heavy metals mobility and bioavailability in contaminated soil using sequential extraction and biosensors, J. Environ. Eng. 135 (2009) 839–844.
[20] X. Zhang, Y. Zhu, E. Elcin, L. He, B. Li, M. Jiang, X. Yang, X. Yan, X. Zhao, Z. Wang, F. Wang, S.M. Shaheen, J. Rinklebe, M. Wells, Whole-cell bioreporter application for rapid evaluation of hazardous metal bioavailability and toxicity in bioprocess, J. Hazard Mater. 461 (2024) 132556.
[21] I.V.N. Rathnayake, M. Megharaj, R. Naidu, Green fluorescent protein based whole cell bacterial biosensor for the detection of bioavailable heavy metals in soil environment, Environ. Technol. Innov. 23 (2021) 101785.
[22] K.B. Riether, M.A. Dollard, P. Billard, Assessment of heavy metal bioavailability using Escherichia coli zntAp::lux and copAp::lux-based biosensors, Appl. Microbiol. Biotechnol. 57 (2001) 712–716.
[23] M.R. Saidur, A.R. Abdul Aziz, W.J. Basirun, Recent advances in DNA-based electrochemical biosensors for heavy metal ion detection: a review, Biosens. Bioelectron. 90 (2017) 125–139.
[24] X. Cao, C. Chen, Q. Zhu, Biosensors based on functional nucleic acids and isothermal amplification techniques, Talanta 253 (2023) 123977.
[25] J. Chen, M. Chen, H. Tong, F. Wu, Y. Liu, C. Liu, Fluorescence biosensor for ultrasensitive detection of the available lead based on target biorecognition-induced DNA cyclic assembly, Sci. Total Environ. 905 (2023) 167253.
[26] W. Zhou, R. Saran, J. Liu, Metal sensing by DNA, Chem. Rev. 117 (2017) 8272–8325.
[27] Y. Zhang, S. Xiao, H. Li, H. Liu, P. Pang, H. Wang, Z. Wu, W. Yang, A Pb^{2+}-ion electrochemical biosensor based on single-stranded DNAzyme catalytic beacon, Sensor. Actuator. B Chem. 222 (2016) 1083–1089.
[28] H. Wang, L. Wang, K. Huang, S. Xu, H. Wang, L. Wang, Y. Liu, A highly sensitive and selective biosensing strategy for the detection of Pb^{2+} ions based on GR-5 DNAzyme functionalized AuNPs, New J. Chem. 37 (2013) 2557–2563.
[29] S. Erbas-Cakmak, S. Kolemen, A.C. Sedgwick, T. Gunnlaugsson, T.D. James, J. Yoon, E.U. Akkaya, Molecular logic gates: the past, present and future, Chem. Soc. Rev. 47 (2018) 2228–2248.

[30] C. Yao, H. Lin, H.S.N. Crory, A. Prasanna de Silva, Supra-molecular agents running tasks intelligently (SMARTI): recent developments in molecular logic-based computation, Mol. Syst. Des. Eng. 5 (2020) 1325–1353.
[31] S. Zhao, L. Yu, S. Yang, X. Tang, K. Chang, M. Chen, Boolean logic gate based on DNA strand displacement for biosensing: current and emerging strategies, Nanoscale Horiz 6 (2021) 298–310.
[32] L. Shi, Q. Tang, B. Yang, W. Liu, B. Li, C. Yang, Y. Jin, Logic-gates of gas pressure for portable, intelligent and multiple analysis of metal ions, Anal. Chem. 95 (2023) 5702–5709.
[33] J. Chen, J. Pan, S. Chen, A label-free and enzyme-free platform with a visible output for constructing versatile logic gates using caged G-quadruplex as the signal transducer, Chem. Sci. 9 (2018) 300–306.
[34] L. Shi, Q. Tang, B. Yang, W. Liu, B. Li, C. Yang, Y. Jin, Dual-mode logic gate for intelligent and portable detection of microRNA based on gas pressure and lateral flow assay, Anal. Chem. 95 (2023) 6090–6097.
[35] Q. Zou, X. Li, T. Xue, J. Zheng, Q. Su, SERS detection of mercury (II)/lead (II): a new class of DNA logic gates, Talanta 195 (2019) 497–505.
[36] W. Deng, J. Xu, H. Peng, C. Huang, X.C. Le, H. Zhang, DNAzyme motor systems and logic gates facilitated by toehold exchange translators, Biosens. Bioelectron. 217 (2022) 114704.
[37] X. Fan, Y. Gao, X. Zhang, J. Li, R. Song, X. Feng, W. Song, "OR" logic gate multiplexed photoelectrochemical sensor for high-risk human papillomaviruses: "One pot" recombinase polymerase amplification and logic discrimination, Talanta 266 (2024) 125090.
[38] F. Deng, J. Pan, Z. Liu, J. Chen, Cascaded molecular logic gates using antibiotics as inputs based on exonuclease III and DNAzyme, Talanta 252 (2023) 123832.
[39] J. Pan, F. Deng, Z. Liu, L. Zeng, J. Chen, Construction of molecular logic gates using heavy metal ions as inputs based on catalytic hairpin assembly and CRISPR-Cas12a, Talanta 255 (2023) 124210.
[40] Z. Li, M. Yang, C. Zhao, Y. Shu, Bifunctional Y-shaped probe combined with dual amplification for colorimetric sensing and molecular logic operation of two miRNAs, Talanta 259 (2023) 124480.
[41] F. Deng, J. Pan, Z. Liu, L. Zeng, J. Chen, Programmable DNA biocomputing circuits for rapid and intelligent screening of SARS-CoV-2 variants, Biosens. Bioelectron. 223 (2023) 115025.
[42] Y. Feng, Y. Yang, Y. Xiao, T. Fu, L. He, L. Qi, Q. Yang, R. Peng, W. Tan, Multi-parameter inputted logic-gating on aptamer-encoded extracellular vesicles for colorectal cancer diagnosis, Anal. Chem. 95 (2023) 1132–1139.
[43] X. Gong, J. Wei, J. Liu, R. Li, X. Liu, F. Wang, Programmable intracellular DNA biocomputing circuits for reliable cell recognitions, Chem. Sci. 10 (2019) 2989–2997.
[44] Z. Wang, J. Yang, G. Qin, C. Zhao, J. Ren, X. Qu, An intelligent nanomachine guided by DNAzyme logic system for precise chemodynamic therapy, Angew. Chem. Int. Ed. 61 (2022) e202204291.
[45] P. Zhou, Y. Pan, W. Pan, S. Lu, J. Yin, N. Li, B. Tang, Dual-AND logic gate-based strip assay for amplified detection of four miRNAs and diagnosis of lung cancer, Anal. Chem. 95 (2023) 1280–1286.